
Proceedings Paper:
Tetlow, L., Rigby, S. orcid.org/0000-0001-6844-3797, Langdon, G. et al. (2 more authors) (2024) Experimental assessment of near-field blast loading using digital image correlation. In: Proceedings of The 19th International Symposium on Interaction of the Effects of Munitions with Structures (ISIEMS). 19th International Symposium on Interaction of the Effects of Munitions with Structures (ISIEMS), 09-13 Dec 2024, Bonn, Germany. International Symposium on Interaction of the Effects of Munitions with Structures (ISIEMS)

Distribution: For public release

Experimental Assessment of Near-Field Blast Loading Using Digital Image Correlation

Lewis Tetlow[1*], Sam Rigby[1], Genevieve Langdon[1], Richard Curry[1], Genevieve Pezzola[2]

School of Mechanical, Aerospace and Civil Engineering, University of Sheffield, Western Bank, Sheffield, United Kingdom

1. School of Mechanical, Aerospace and Civil Engineering, University of Sheffield, UK

2. U.S. Army Engineer Research and Development Center, USA

Keywords: Blast, Experimental Investigation, Blast Propagation

Abstract

This paper presents an experimental study of a 400x400mm 1mm thick aluminium plate loaded by an explosive charge at three different stand-off distances (100, 150 and 300 mm). The back face of the plate is optically captured with high-speed video at a frame rate of 100,000fps and digital image correlation (DIC) post-processing is used to determine temporal displacement and velocity. This is recorded at approximately 2,200 data points across the plate surface, which results in a resolution of experimental data that is typically challenging to achieve, due to the near-instantaneous application of high magnitude loading. The velocity information is used to infer a specific impulse value for each individual data point and can therefore determine a spatial loading profile.

The results show that closer stand-off distances result in an increased localisation and magnitude of loading. The spatial variation of specific impulse is shown to be significant enough that idealised Gaussian loading curves do not sufficiently represent the loading anomalies evident in near-field loading. The amount of data generated from each individual test allows a probabilistic approach that considers loading as a ‘banding’ rather than single idealised distribution for each stand-off. It is only with an appreciation of the spatial variability of loading magnitude and experimental data of this resolution that we can accurately simulate the real-world features of near-field blast loading.

Introduction

Close-proximity blast loads are characterised by extreme magnitudes of pressure and impulse, occurring over timescales measured in milliseconds [10]. Traditional design methods derived from UFC blast-load parameter predicative curves have been found to underestimate the magnitude of loading at short stand-off distances [9]. The extreme pressures and short timescales also mean that experimental assessment of blast parameters is difficult, limiting the ability of blast engineers to validate numerical solvers and computational fluid dynamic codes.

Structures that are designed to resist loading of this sort must also contend with a degree of spatial complexity that is not present when subjected to blast loading from a greater stand-off distance [4]. In a simplistic case, where the blast wave is considered as an outwardly propagating sphere, smaller stand-off distances result in a more centrally localized loading profile applied to a target structure. Furthermore, when stand-off distances fall within the so-called near-field (scaled distances of approximately less than 2 m/kg$^{1/3}$), the detonation product cloud (DPC) is still interacting with the shockwave, which is present as a shell of compressed air attached to and being driven outward by the DPC.

Several studies have found that anomalies, protrusions and fluid-dynamic instabilities form within the fireball as it propagates outwards [2, 6, 10]. Rigby et al. [6] further sub-categorised the near-field into two regions based upon the fireball/DPC shape irregularity. In the early time near-field, the DPC shape is more idealised as anomalies and instabilities haven't had sufficient time to develop and tangibly affect the fireball. However, in the later time Rigby et al. [6] notes how the anomalies become more developed and cause the DPC to have a far less regular and more variable profile.

It is clear that DPC anomalies could affect the spatial characteristics and variation of near-field blast loading. If we are to fully understand these spatial and transient features of near-field blast loading and adequately design against close-proximity explosive events, accurate measurement of near-field blast loading parameters is required. This study presents an experimental methodology developed from Rigby et al. (2019a), which uses digital image correlation (DIC) instrumentation to determine the loading profile impinging on a structure. This approach has been adapted further to focus upon determining spatial loading profile within the near-field range of scaled distances at a high fidelity.

Experimental Setup

The experimental testing for this paper comprised a thin square plate loaded by the detonation of an explosive charge at three discrete stand-off distances (within the near-field range). The plates were 400x400mm, clamped within a frame that leaves a 300x300mm exposed area and composed of 1mm thick Aluminium 1050 series (the plate and clamping frame schematics are illustrated in Figure 2).

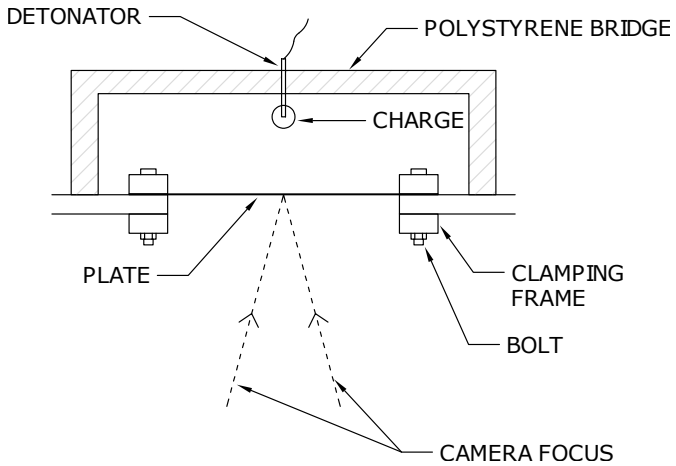

Figure 1. General arrangement of charge placement relative to the plate, clamping frame and camera focus point.

The plate was painted with a white primer and a speckle pattern was applied for use within the digital image correlation post-processing (as shown in Figure 3). A stereo pair of Photron SAZ high speed video cameras were focused upon the rear face of the plate and synced using Correlated Solutions VIC 3D software. The cameras recorded at a frame rate of 100,000fps and a resolution of 640x280 pixels.

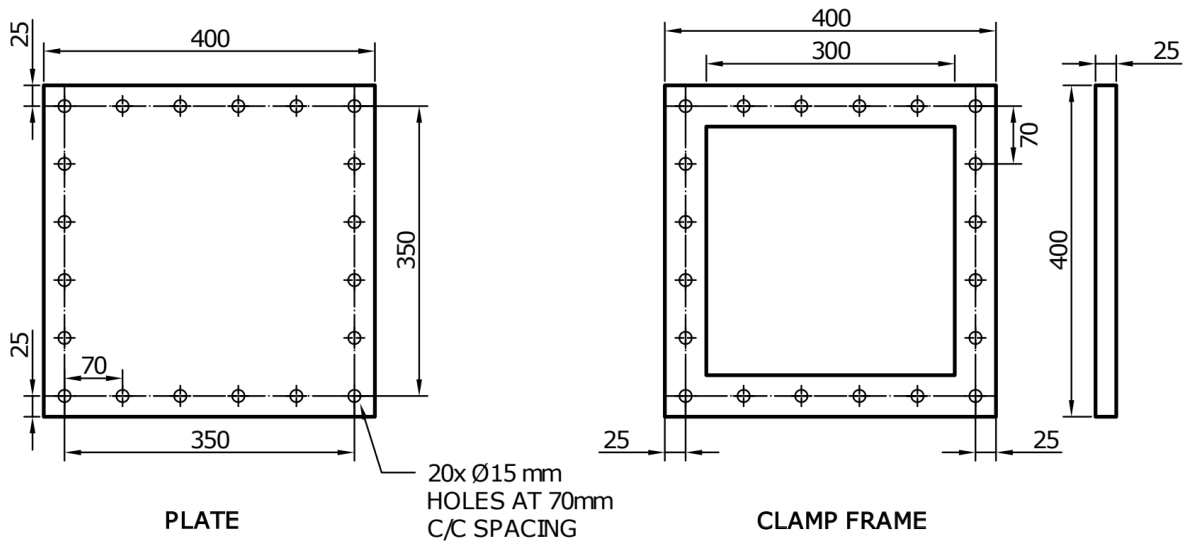

Figure 2. Plate and clamp frame schematic.

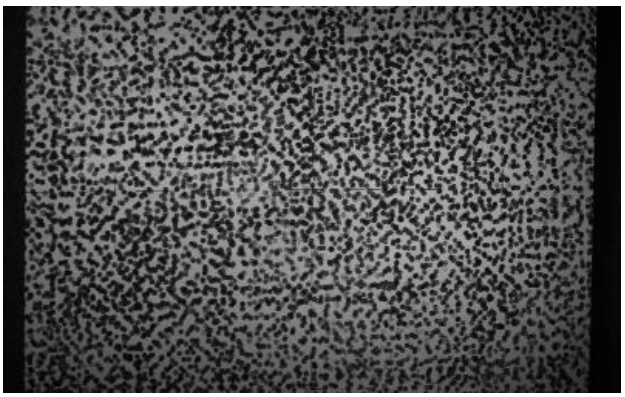

Figure 3. Image of speckle pattern painted onto the plate rear face for use within the DIC algorithm.

Explosive charges comprised 25g PE10 spheres shaped using 3D printed moulds. Non-electric 0.8g (TNT equivalent) detonators were used, located centrally within the charge. Positioning and stand-off distance was achieved using a “bridge” structure made of polystyrene, selected to minimize loading reflections from the mounting structure. The three test setups referenced within this paper are summarized in Table 1.

Test Ref	Stand-Off Distance	Charge Mass	Charge Shape	Scaled Distance
-	mm	g	-	m/kg^1/3
A	100			0.342
B	150	25	Sphere	0.513
C	300			1.026

Table 1. Test information for the experimental set-ups used. Scaled distance is calculated using the mass of PE10 excluding the detonator.

Digital Image Correlation

Digital Image Correlation (DIC) is a post-processing tool that generates full field positional and displacement data for each frame of a given recording. It does this by splitting a target surface into a series of square subsets of a specified pixel size, which both cameras are able to identify. For each subset the two cameras identify its position within the frame of reference and then use a calibration algorithm to determine global position.

Confidence of the 'match' between the two cameras is determined by the speckle pattern applied to the surface which needs to be unique for each individual subset. This is determined by the points of high contrast (i.e. black-to-white) between pixels, the pattern of which needs to be suitably stochastic and dense (Correlated Solutions, 2024). As this study focuses upon the high-speed application of DIC, where exposure time is short, the lighting of the target surface had to be maximised to highlight contrast in the speckle pattern.

Calibration of the DIC algorithm was achieved using Correlated Solutions proprietary calibration boards which were recorded in individual images positioned across the entire frame of interest. Images were captured prior to testing and the resultant calibration is used to determine the position of each subset, yielding both a position-time and displacement-time histories at each specific subset. Additionally, velocity data can be computed using recorded frame rate of the cameras giving a velocity-time history. Examples of the recorded displacement and velocity histories averaged over the central 10mm of the plate are shown in Figure 4 for each of the three test stand-offs captured.

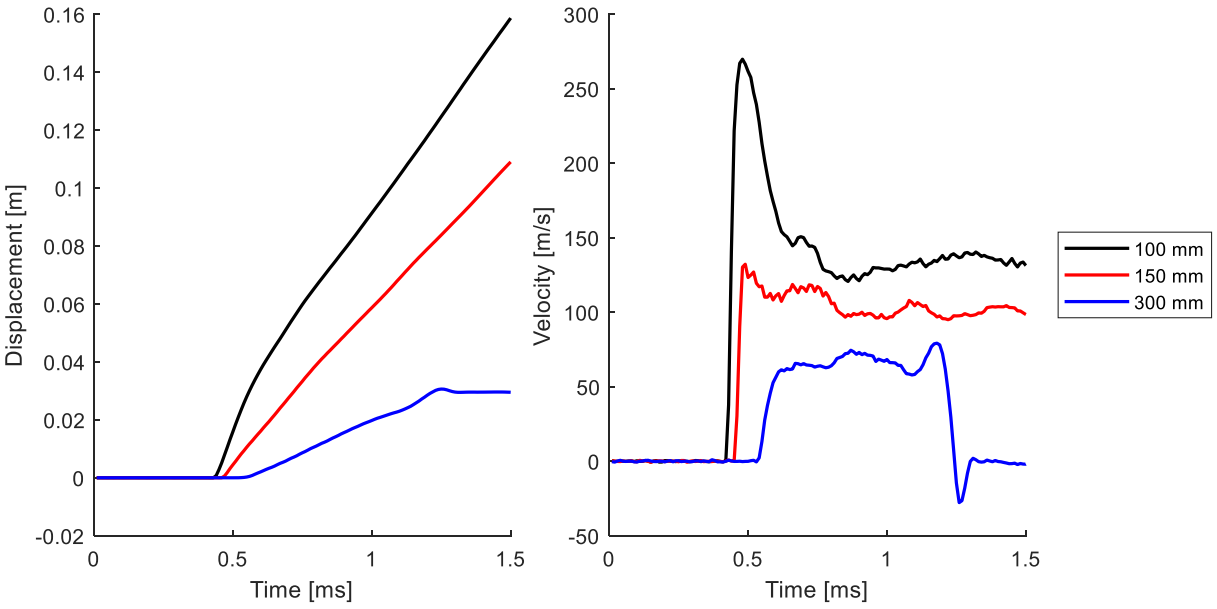

Figure 4. Displacement and velocity time histories averaged over the central 10mm of the plates for each stand-off distance.

Results and Discussion

Figure 4 shows both the displacement history and the velocity history for the 3 test stand-off distances (SOD) averaged over the central 10mm of the plate. During Tests A and B the plate underwent complete tearing at the clamping boundary (Mode II failure) which is evident in the in the near linear displacement-time responses in Figure 4a and the continuous plateau in velocity in Figure 4b. Test C however remained in the clamping frame, resulting in the displacement plateau after 1.2ms.

The velocity plot for Test C also shows a sharp increase then immediate deceleration to negative velocity before resolving to zero. This is the result of a region plasticity migrating inwards from the plate boundary, which transforms the remaining kinetic energy in the plate at a given point into plastic deformation and leaves the plate nominally at rest thereafter. By plotting velocity contours across the 2D surface of the plate, the plastic hinge inwards migration with time can be seen more clearly (Figure 5).

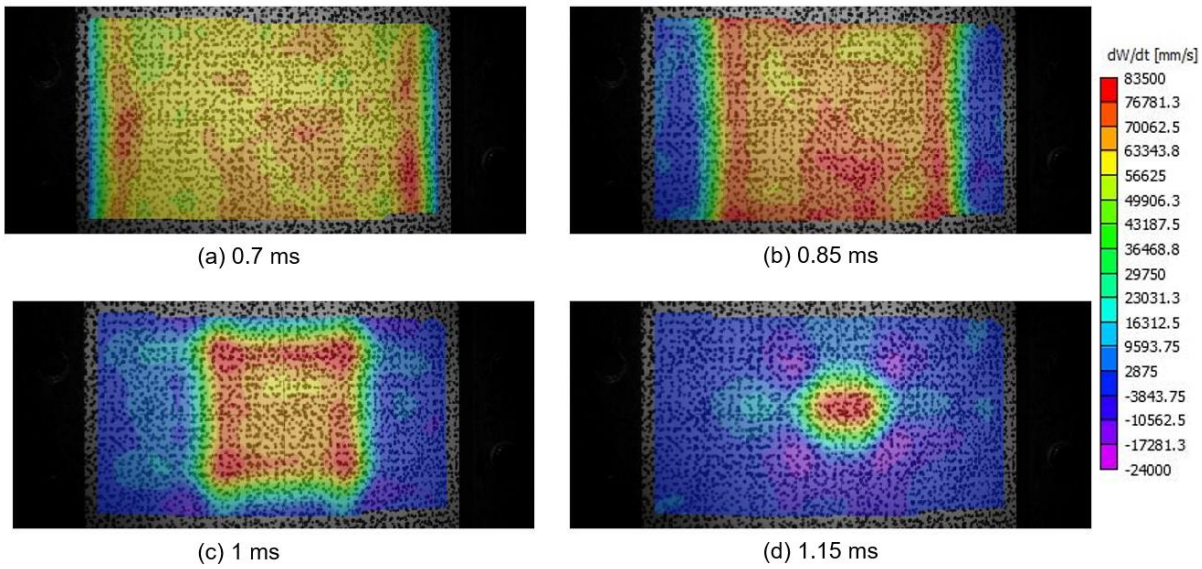

Figure 5. Velocity contour plots at increasing times showing the inwards translation of the plastic hinge.

The initial velocity uptake of the plate centre in Figure 4b is seen to be a rapid rise for all three SOD, however test C appears to be more gradual. Test A (closest SOD) has a distinct peak in velocity highlighted by a rapid deceleration after its initial rise. This behaviour is likely caused by a higher localisation of central loading resultant from the closer stand-off distance. This was also evident in the final deformation profile of the plate which exhibited a central dome additionally to the global dome of the plate, which is consistent with a more localised loading profile 1, 3].

The velocity histories of data-points across the plate are also a representation of the plate's momentum which is in-turn determined by the impulse applied. Specific impulse across the plate can be determined using this understanding alongside the rationalisation of the plate into a series of discrete masses with no shear resistance between adjacent masses. This methodology was demonstrated by Rigby et al. [5] and has been altered in this study to improve the resolution and spatial detail of the loading with the purpose of capturing complex loading features and fluctuations.

If the applied loading is assumed impulsive then the velocity uptake of the plate is considered to be near instantaneous. However, different sections of the plate will experience loading at different times due to the localisation and geometry of the outwardly propagating blast wave. The peak of the first rapid rise in the velocity-time histories seen in Figure 4b is considered to be the resultant initial velocity caused by the loading. Caution is required, however, to ensure that aspects of the velocity profile directly resulting from the applied load are separated from the ensuing structural response. For

example, it is important to avoid the later velocity peak caused by the plastic hinge seen in Test C in Figure 4 being sampled as the velocity used to determine the loading. This is because the travelling hinge behaviour is a function of the structure rather than the loading and will result in incorrectly inferred loading and impulses if this peak is used.

Once the peak velocity is determined for each data-point of the DIC data, it can then be multiplied by the spatial density (plate thickness multiplied by density) to give a value of peak momentum for that point which is equivalent to a specific impulse for that data-point. This yields a full-field loading distribution, demonstrated in Figure 6 which shows specific impulse value of each data point across the three tests plotted against its radial distance from the plate centre.

Figure 6 shows the reduction in stand-off distance results in an increase in central magnitude of loading but also central localisation. What is clear for all three curves is that the loading profile inhabits a banding of loading with radial distance and that they each exhibit non-idealised features. Each curve fluctuates away from an idealised Gaussian curve that is traditionally outputted from CFD solvers or near-field models [4]. This is most notable in areas of obvious increase or peaks in loading: Test A - centrally and ~70mm; Test B - ~40mm, 70mm and prominently above 100mm; Test C – ~ 120mm.

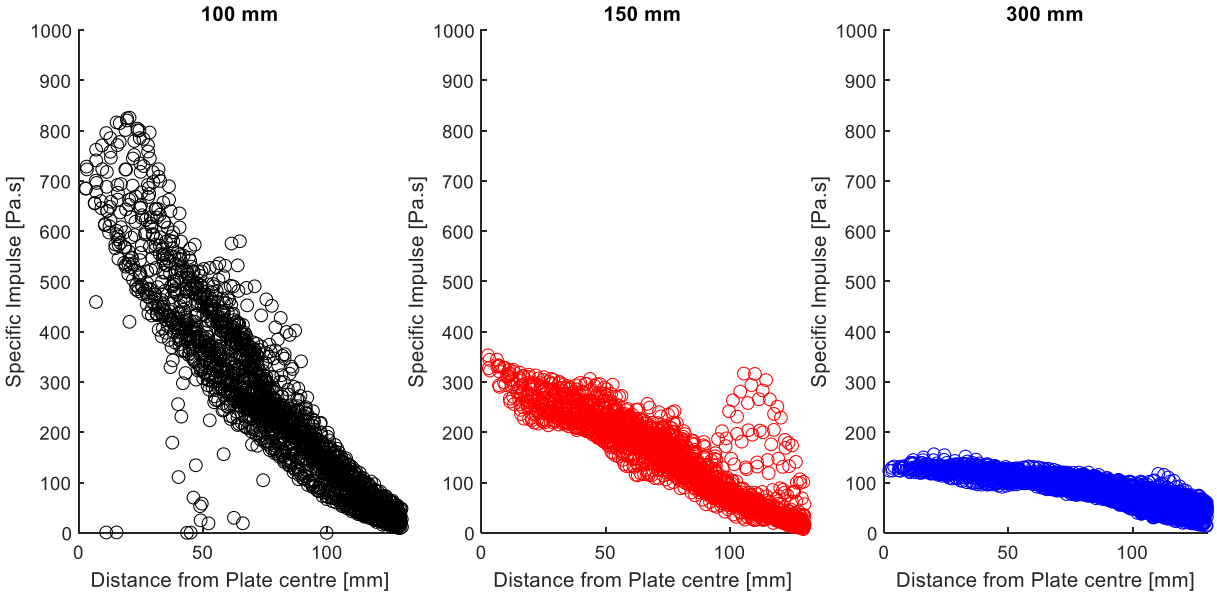

Figure 6. Radial specific impulse extracted from each data point (subset) extracted from the DIC post-processing.

The plots in Figure 6 show the high density of loading data-points generated from a single test. This makes it difficult to visualize the extent of fluctuation or imperfections in the loading profile. However, the number of data points means that this information can be analysed probabilistically. To do this the radial distance out from the plate centre was segmented into bands 5mm wide and the points within each band are sampled as an individual probability distribution. For each band the mean values of specific impulse and the standard deviation were computed. Figure 7 plots the mean specific impulse distribution with the first standard deviation banding of loading shaded either side (i.e. mean plus or minus 1 standard deviation).

Figure 7 encompasses 67% of the recorded loading values and gives a more concentrated representation of the loading structures recorded by the DIC experiments. It accurately represents the peaks and fluctuations in the loading and with further tests this probabilistic approach can be used for a data driven approach to predicting near-field blast loading at a high spatial resolution. What is clear from both Figure 6 and 7 is that near-field loading can't be considered in an idealised sense that neglects the inherent variability in the loading. The specific impulse distribution applied to a target structure must instead be considered as a banding if the true spatial characteristics are to be accounted for.

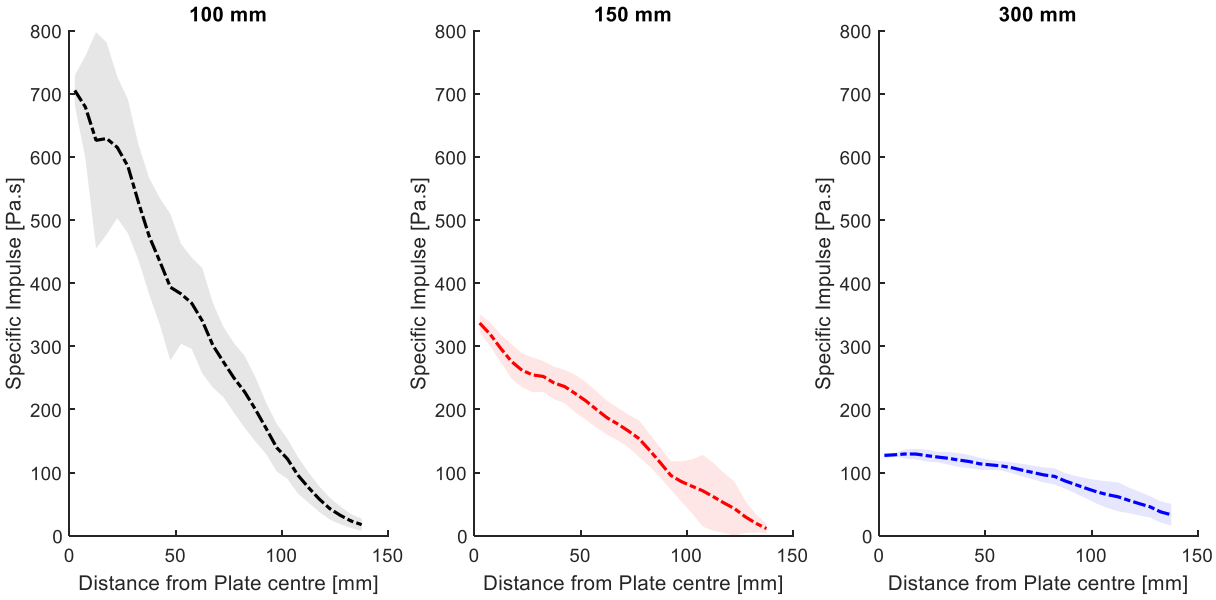

Figure 7. Mean radial specific impulse with the first standard deviation range indicated in the shaded region.

Conclusion

This study has presented an experimental study of a blast loaded plate within the near-field at three discrete stand-off distances, at or below a Hopkinson-Cranz scaled distance of 1 m/kg$^{1/3}$. The methodology uses digital image correlation post-processing in conjunction with high-speed video footage captured at 100,00fps. It has been demonstrated how this methodology can infer a loading distribution at an extremely high resolution, considering the speed and magnitude of loading at such small stand-off distances.

The results show an obvious trend of increased magnitude and localisation of the loading distribution as stand-off distance reduces. However, multiple cases of spatial fluctuation and variability in specific impulse magnitude are seen across all three tests. This is at odds with the traditionally idealised Gaussian curves used to represent loading at this SOD, typically generated from CFD solvers or low-resolution experimental data. Furthermore, the spread of results demonstrate that the spatial loading must be considered as a ‘banding’ and one single idealised curve is not sufficient to accurately represent near-field loading. Figure 7 demonstrated that the significant number of data points captured by this experimental methodology enables a probabilistic approach that engineers can use to more realistically predict and simulate near-field blast loading if supplemented with repeat tests. It is only with experimental approaches at this resolution that we can accurately model the loading structures and anomalies present in near-field blast loading.

Acknowledgements

The first author acknowledges the support of the U.S. Army Engineer Research and Development Center in funding this project.

References

1. Chung Kim Yuen, S., Nurick, G. N., Langdon, G. S. & Iyer, Y. (2017), 'Deformation of thin plates subjected to impulsive load: Part III – an update 25 years on', International Journal of Impact Engineering 107, 108–117.
2. Fuller, B., Rigby, S., Tyas, A., Clarke, S., Warren, J., Reay, J., Gant, M. & Elgy, I. (2016), Experimentation and modelling of near field explosions, in '*Proceedings of the 24th Military Aspects of Blast and Shock*', Halifax, Nova Scotia, Canada.
3. Nurick, G. & Radford, A. (1997), 'Deformation and tearing of clamped circular plates subjected to localised central blast loads', Recent developments in computational and applied mechanics: a volume in honour of John B. Martin pp. 276–301.
4. Pannell, J. J., Panoutsos, G., Cooke, S. B., Pope, D. J., & Rigby, S. E. (2021). Predicting specific impulse distributions for spherical explosives in the extreme near-field using a Gaussian function. *International Journal of Protective Structures*, *12*(4), 437–459. https://doi.org/10.1177/2041419621993492
5. Rigby, S. E., Akintaro, O. I., Fuller, B. J., Tyas, A., Curry, R. J., Langdon, G. S. & Pope, D. J. (2019b), 'Predicting the response of plates subjected to near-field explosions using an energy equivalent impulse', International Journal of Impact Engineering 128, 24–36.
6. Rigby, S. E., Knighton, R., Clarke, S. D. & Tyas, A. (2020), 'Reflected Near-Field Blast Pressure Measurements Using High Speed Video', Experimental Mechanics 60(7), 875–888.
7. Rigby, S. E., Tyas, A., Clarke, S. D., Fay, S. D., Reay, J. J., Warren, J. A., Gant, M. & Elgy, I. (2015), 'Observations from preliminary experiments on spatial and temporal pressure measurements from near-field free air explosions', International Journal of Protective Structures 6(2), 175–190.
8. Rigby, S. E., Tyas, A., Curry, R. J. & Langdon, G. S. (2019a), 'Experimental Measurement of Specific Impulse Distribution and Transient Deformation of Plates Subjected to Near-Field Explosive Blasts', Experimental Mechanics 59(2), 163–178.
9. Shin, J., Whittaker, A. S., & Cormie, D. (2015). Incident and Normally Reflected Overpressure and Impulse for Detonations of Spherical High Explosives in Free Air. *Journal of Structural Engineering*, *141*(12), 04015057. https://doi.org/10.1061/(asce)st.1943-541x.0001305
10. Tyas, A. (2019). Blast loading from high explosive detonation: What we know and don't know. *13th International Conference on Shock and Impact Loads on Structures, SILOS 2019*, 13–15.